JOURNAL OF GEOPHYSICAL RESEARCH, VOL. 95, NO. C10, PAGES 18,281–18,288, OCTOBER 15, 1990

Bubble-Mediated Aerosol Production as a Consequence of Wave Breaking in Supersaturated (Hyperoxic) Seawater

MAŁGORZATA STRAMSKA, ROMAN MARKS, AND EDWARD C. MONAHAN

Marine Sciences Institute, University of Connecticut, Avery Point, Groton

The influence of changes in the degree of saturation of the surface waters, with respect to the major atmospheric gases, on the aerosol productivity of an individual whitecap has now been inferred from results recently obtained using the University of Connecticut's Whitecap Simulation Tank IV. As the level of dissolved oxygen increased from 100% saturation to 130%, i.e., to a significant degree of supersaturation, the production of aerosol droplets by the whitecap generated by a standard laboratory breaking wave was found to increase by a factor of 2.4 in the case of submicron radius droplets, while the generation of larger droplets ($r > 2.5$ μm) was observed to increase by at least a factor of 4.0. As a consequence of these findings, a multiplier, defined in terms of the degree of gas saturation, has been introduced as a term in the various sea surface aerosol generation models.

INTRODUCTION

It has also long been recognized that wave breaking gives rise to bubbles in the near surface waters of the ocean [*Jacobs*, 1937]. It has also long been conjectured that surface waters supersaturated with respect to the major constituent gases of the atmosphere might effervesce [*Blanchard and Woodcock*, 1957, 1980].

The possibility that a wave breaking in markedly supersaturated sea water might result in many more bubbles rising to the air-sea interface than would be found rising to this surface if an identical breaking wave had occurred in saturated seawater has not been considered in detail. *Thorpe* [1982] does discuss the fate of individual gas bubbles for seawater saturations ranging from 96% to 110% in his detailed treatment of the role in air-sea gas exchange of the bubble plumes that are formed when waves break. *Garbalewski and Marks* [1985], in discussing the relatively high concentration of marine aerosol particles they measured in the summer over the sea near Antarctica, suggested that the substantial oxygen supersaturation of these surface waters as well as the gustiness of the wind may have contributed to an enhanced emission of marine aerosols from the sea surface.

The present study was conducted to determine what effect, if any, the degree of saturation of seawater with respect to the major atmospheric gases has on the number and the size distribution of the droplets produced during the decay of an individual oceanic whitecap. If this effect is a pronounced one, then given the prevalence of surface waters markedly supersaturated with dissolved oxygen and by inference dissolved nitrogen in certain extensive oceanic regions such as the southern ocean [*Gordon and Molinelli*, 1986] at certain times of year, there is reason to conclude that the various models that explicitly relate the aerosol flux up from the sea surface [e.g., *Monahan et al.*, 1982, 1986; *Stramska*, 1987; *Woolf et al.*, 1988] and the related flux of bubbles up to that surface [*Monahan*, 1988*a*, *Monahan and Woolf*, 1989] to oceanic whitecap coverage needs to be refined by the introduction of a multiplier, defined in terms of the degree of gas saturation, into the several mathematical expressions used to formally describe these models. This multiplier can in turn be used to estimate more accurately the various global fluxes. The full implementation of any such refined models will require more geographically and seasonally comprehensive data on dissolved gas saturation levels than are presently available.

Paper number 90JC00667.
0148-0227/90/90JC-00667$05.00

EXPERIMENTS

All of the measurements discussed in this paper were obtained by producing, by means of wave-wave interactions, whitecaps in the 3.0-m-long whitecap simulation tank (WST) depicted in Figure 1. Among the salient features of this laboratory system was the provision to fill, and refill as required, the Plexiglas tank with $2\frac{1}{4}$ m^3 of seawater of salinity of approximately 30‰ drawn from adjacent Long Island Sound. The air over the water in this system was enclosed by a Plexiglas hood, which could readily be placed over or removed from the tank proper by means of an overhead gantry. As can be seen in Figure 1, the hood used in the present experiments was equipped with ports at either end and with four small fans oriented so as to induce a counterclockwise circulation of the air within the hood. As a result of this circulation and the associated enhanced levels of turbulence, the air within the hood and above the water in the tank was well mixed. The standard experimental protocol adopted for the present study required that prior to each breaking wave event air be blown into one port of the hood via a tandem pair of Vokes high-volume air filters and allowed to escape out of the other port until the concentration within the hood of all aerosol particles with radii greater than 0.25 μm was reduced to less than 1.5×10^6 m^{-3}, at which point the intake blower was shut off, the outlet port was capped, and a wave-wave interaction event was triggered.

The mechanism used to generate the two opposite-directed solitary waves whose collision resulted in a whitecap and its associated subsurface bubble plume is illustrated in Figure 2. This system was adopted because it generated reproducible breaking wave events, and hence standard whitecaps. The particular geometry of these twin channels was selected so as to replicate in all significant respects the dimensions of the side channels incorporated in the earlier

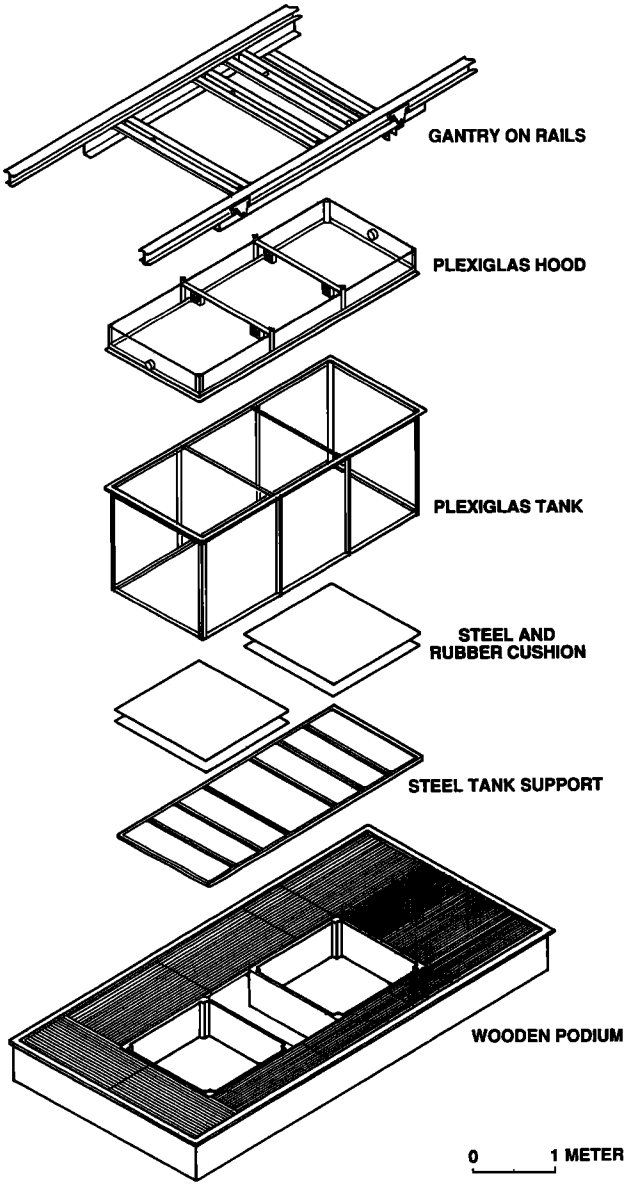

Fig. 1. Exploded view of whitecap simulation tank IV, shown with its podium, hood, and gantry. See text for details.

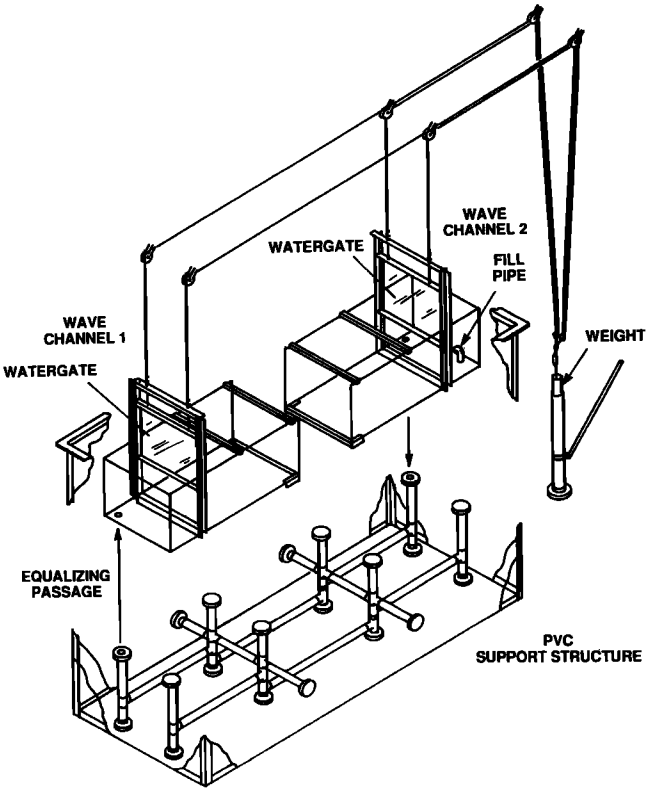

Fig. 2. Twin elevated channels, with watergates, used in Whitecap Simulation Tank IV to generate two opposite-directed waves that collide and give rise to bubbles and aerosol droplets. See text for operating particulars.

whitecap simulation tank (WST II) used in an extended series of aerosol generation experiments, beginning with those conducted by *Monahan et al.* [1979] a decade ago. This choice was made to facilitate the direct intercomparison of the results obtained previously with WST II with the findings now being generated using the new tank (WST IV).

Before each breaking wave event, water was pumped from the bottom of WST IV into the extreme right-hand end of the right channel or sluice, that portion of this channel being temporarily sealed off and made watertight by means of the right water gate. The pumping continued until the water level behind the right gate had reached an elevation of 0.27m above the bed of the right sluice. The water level behind the lowered water gate in the left channel was simultaneously brought to the same elevation by means of piping that interconnects the far ends of both channels. Then, the general level of the seawater in the tank and in the open sections of both channels was 18 mm above the elevation of the sluice beds, and 0.61m above the bed of the tank. In order to start the two waves heading simultaneously toward the center of the tank, it was necessary only to pull the handle allowing the weight, shown at the extreme right of Figure 2, to drop. The fall of this weight, via the action of wires running over pulleys, caused the two water gates to be raised simultaneously, releasing the pent-up masses of seawater. Sketches showing the sequence of events from water gate withdrawal to bubble plume production are given by *Monahan* [1986] and *Cipriano et al.* [1987]. These figures, prepared to illustrate whitecap generation in WST II are equally applicable to WST IV. Not only were the wave generating mechanisms identical in the two whitecap simulation tanks, but the initial water levels behind and in front of the water gates were the same for the experiments carried out in both tanks.

The aerosol concentrations within the hood of WST IV were measured with a Royco model 225 aerosol particle counter equipped with a model 519 plug-in module. The accompanying model 241 optical sensor unit was placed above the hood, with the air being drawn into this unit via a small gland in the hood's top surface by means of an air sampling tube of 2.0-m length, or in some instances, 0.85-m length. The open end of this tube was held at one of several selected elevations and at one of a set of fixed horizontal locations, by means of an adjustable Plexiglas frame. The aerosol measurements were recorded continuously over an interval extending from a minute or more before each breaking wave event to several minutes after the decay of the resulting whitecap.

The dissolved oxygen concentration in the seawater was

recorded for each breaking wave event using a Yellow Springs Instrument Company model 58 dissolved oxygen meter, the probe for which was suspended at intermediate depth in the tank. The relative humidity and temperature of the air beneath the hood and the temperature of the seawater were routinely recorded as well. The seawater temperatures associated with the various breaking wave events discussed in the following section ranged from 12.9°C to 23.5°C.

Aerosol measurements were made in conjunction with some 637 breaking wave events carried out as part of the initial set of transient whitecap experiments conducted using WST IV. A subset of these aerosol recordings, those obtained during 164 breaking wave events for which it was clear that large drops (the spume drops generated by the direct interaction of the two colliding waves) did not contaminate the Royco optical probe and for which the near-neutral or only slightly stable stratification of the air beneath the hood (as reflected in the air-water temperature difference), combined with the action of the hood fans, guaranteed a quite rapid approach to near-homogeneous distribution of the smaller aerosol droplets within the entrapped volume of air, were selected for the analysis described in the following section of this paper.

RESULTS

The increase in the concentration within the hood of bubble-produced droplets immediately subsequent to a breaking wave event was found to depend strongly on the degree of oxygen saturation of the seawater. This can be seen clearly in the strip chart recorder tracings reproduced in Figure 3. In Figures 3*a* and 3*b* the upper, high-amplitude traces were obtained from breaking wave event 398, which was produced in seawater that was 119.1% saturated with respect to oxygen, while the lower, smaller-amplitude traces resulted from breaking wave event 373A, which was generated when the seawater was only 90.4% saturated with respect to oxygen. All sampling was done with the intake end of the 2.0-m tube at an elevation of 0.45 m over the central portion of the tank.

The trace reflecting the concentration of all droplets with radii greater than 0.25 μm that resulted from a breaking wave in seawater 90.4% saturated with oxygen (lower trace, Figure 3*b*) shows that the number of these droplets increased rapidly from the instant the wave broke, and reached a maximum value within a few seconds. The character of this trace, which is typical of the strip-chart recordings obtained when the air that was sampled by the Royco optical sensor was drawn from above the central well formed by the gap between the two wave channels, is consistent with the interpretation that most of these droplets having radii greater than 0.25 μm are film droplets and hence are generated primarily from the rupture of the film caps of the largest bubbles, which are the first to rise to the surface and burst [*Woolf et al.*, 1987]. The slow subsequent decrease with time in the amplitude of this trace reflects the slow loss of these small droplets by sedimentation and other processes. The small but measurable pre-breaking-wave concentration recorded at the beginning of this trace, amounting to less than 5×10^5 m^{-3}, i.e., to less than one particle per milliliter is a measure of the residual, primarily nonmarine, aerosol loading carried by the air as it entered the hood after passing through the tandem Vokes air filters.

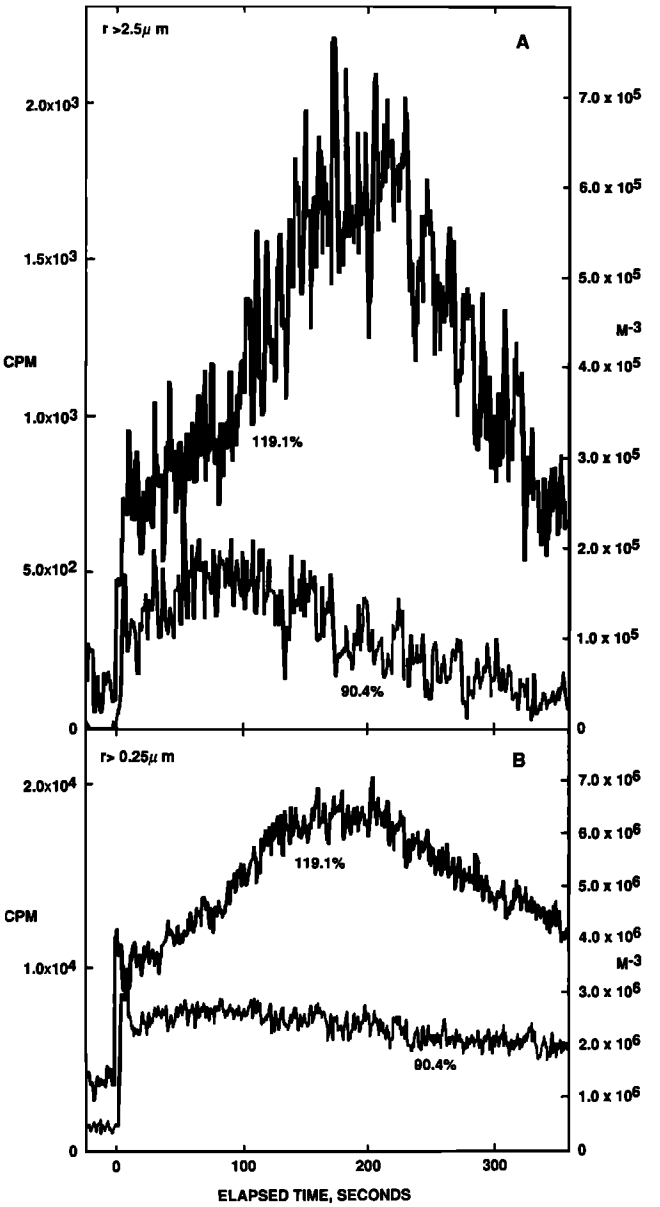

Fig. 3. Replicas of four strip-chart traces of output from the Royco model 225 aerosol particle counter. Each trace shows increase in aerosol concentration within the hood of WST IV subsequent to wave breaking at time 0. The left-hand vertical scale indicates the Royco counts per minute, while the right-hand vertical scale shows the concentration of particles per cubic meter. (*a*) Concentration of droplets with radii greater than 2.5 μm, as recorded during breaking wave events 373A (oxygen saturation level of 90.4%) and 398 (119.1% oxygen saturation). (*b*) Concentration of droplets with radii greater than 0.25 μm, as recorded during same two breaking wave events.

In marked contrast, the trace detailing the concentration of the larger aerosol particles (radii > 2.5 μm) as a function of time from the instant of wave breaking in 90.4% saturated sea water (lower trace, Figure 3*a*), increases only slowly in amplitude, not reaching a maximum until approximately a minute after the wave broke. This behavior is in accord with the contention that these larger particles are almost exclusively jet droplets [*Woolf et al.*, 1987] and as such owe their origins to the Worthington jets produced upon the collapse of the cavities left behind when the smaller, slowly rising

bubbles reach the air-water interface and burst [*Kientzler et al.*, 1954]. Most of the progenitor bubbles responsible for these droplets were less than 100 μm in radius. The subsequent decline with time in the amplitude of this trace, which is more rapid than the fall-off of the previously discussed trace, is a consequence of the higher gravitational fall velocities associated with these larger droplets. It is to be noted that the presplash background concentration of aerosol particles with radii greater than 2.5 μm is essentially zero, reflecting the successful removal of all larger-than-micron radius particles from the incoming air by the Vokes filters.

The two traces described earlier are qualitatively similar to the sets of comparable traces obtained when numerous breaking wave events were produced in seawater that was near saturation or undersaturated with respect to oxygen.

The trace depicting the evolution of the concentration within the hood of jet droplets in that instance where the breaking wave occurred in water 119.1% saturated with respect to oxygen (upper trace, Figure 3*a*) implies that these droplets were produced over an interval extending for several hundred seconds after the wave broke, documenting a much more prolonged jet droplet generation interval than was observed when the water was only 90.4% saturated (lower trace, Figure 3*a*) and mirroring the fact that many small bubbles were still arriving at the water surface several minutes after the breaking wave event. The maximum jet droplet concentration obtained in this supersaturated case is several times as great as the maximum concentration recorded for the undersaturated case. It should be noted that the jet droplet trace corresponding to supersaturation reflects a small but finite background, or presplash, concentration (approximately 5×10^4 m^{-3} in the case of breaking wave event 398), from which it can be inferred that there was a discernible flux of small bubbles striking the water surface prior to this particular breaking wave event.

The final trace replicated in Figure 3, that showing the concentration of small aerosol droplets (those with radii >0.25 μm) as it evolves with the passage of time subsequent to a wave breaking in supersaturated sea water (upper trace, Figure 3*b*), indicates that after the initial spurt of film droplets there was a protracted period during which significant numbers of additional film droplets and small jet droplets were produced as a consequence of the delayed arrival at the water surface of many small bubbles. The maximum concentration attained by these small droplets within the hood in the supersaturation case (upper trace, Figure 3*b*) was about twice the maximum small-particle concentration encountered in the undersaturated case (lower trace, Figure 3*b*), but the ratio of these maximum small droplet concentrations is considerably less than the ratio of the maximum jet droplet concentrations as inferred from the two traces reproduced in Figure 3*a*. The presplash small-droplet concentration in the case of supersaturated seawater was greater than the background small-particle concentration measured in the case where the seawater was undersaturated with respect to oxygen, again reflecting the aerosol contribution arising from the presplash flux of surfacing bubbles.

The two traces recorded when the seawater was 119.1% saturated, and included in Figure 3, are typical of the many aerosol traces which were obtained when breaking waves were generated in supersaturated seawater.

It is of particular interest to know the total number of sea spray droplets produced for the various levels of seawater oxygen saturation as a consequence of a standard breaking wave event. This quantity can be determined for the two droplet size categories described earlier from the analysis of individual time series of droplet concentrations recorded for the numerous breaking wave events, such as those shown in Figure 3. In the case of a trace such as the lower one in Figure 3*b*, the initial high narrow peak is ignored, as it occurred at a time when the aerosol droplets were not yet well mixed beneath the hood of WST IV, and the average concentration recorded for the following few tens of seconds, minus the presplash background concentration, is taken as a measure of the uniform increase in the concentration throughout the entrapped air that resulted from the particular breaking wave event. This change in concentration, multiplied by the volume of air contained beneath the hood of WST IV, which is 3.01 m^3 for the water level used throughout these experiments, yields the estimate of the number of droplets generated as a consequence of that breaking wave event. Estimating the droplet production associated with traces such as the other three included in Figure 3 is a considerably more difficult task. In the case of traces such as these it is necessary first to estimate, from the postproduction portion of each trace, the fractional decrease in concentration per unit time that occurs owing to sedimentation and other processes. Then from a consideration of the prepeak portion of each trace, the cumulative loss of droplets, and hence the total decrease in concentration due to sedimentation, up to the time of the peak needs to be assessed, and the peak concentration duly augmented to account for these losses. Once this adjusted peak concentration has been determined, the estimate of the droplet production associated with the particular breaking wave event proceeds as in the previous example; i.e., the adjusted peak concentration minus the presplash background is multiplied by the volume of air beneath the hood to arrive at the desired number.

In Figure 4 the total number of droplets with radii greater than 0.25 μm generated by each of the 164 selected standard breaking waves is plotted against the percentage oxygen saturation of the seawater in which the breaking wave occurred. Results obtained both from measurements made when the air samples were drawn into the Royco counter through 0.85-m and 2.0-m intake tubes are shown. The strong increase in the number of droplets produced associated with increasing levels of dissolved oxygen is apparent. These combined data can be described by

$$N(r > 0.25\mu m) = 5.54 \times 10^5 \exp(+0.0291s) \quad (1)$$

where s is the percentage oxygen saturation of the seawater. The correlation coefficient for this fit to these data is 0.96. The number of jet droplets with radii greater than 2.5 μm produced by each of these same 164 breaking wave events is plotted as a function of percentage oxygen saturation in Figure 5. The marked positive dependence of jet droplet production on oxygen saturation levels is reflected in the following equation, which describes these data with an associated correlation coefficient of 0.83.

$$N(r > 2.5\mu m) = 1.025 \times 10^4 \exp(+0.0470s) \quad (2)$$

The growth of jet droplet generation with increasing levels of oxygen saturation is more rapid than the growth with in-

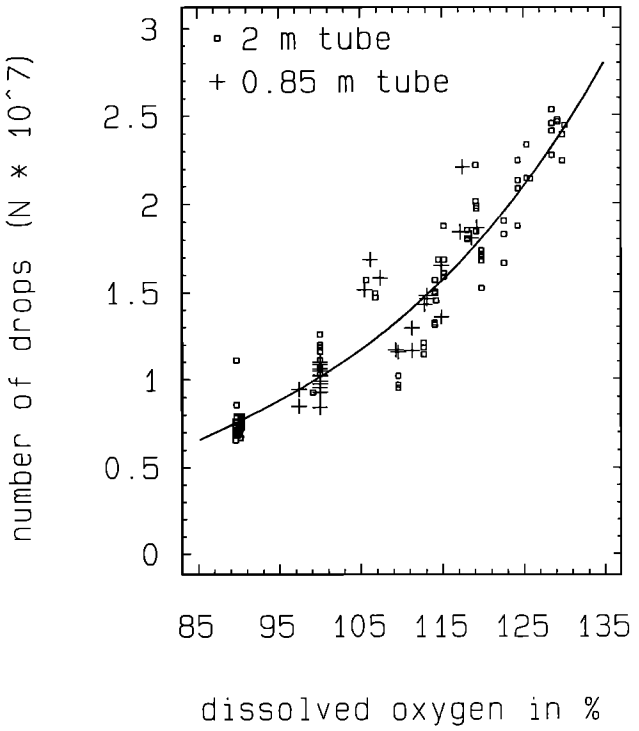

Fig. 4. Total number of droplets with radii greater than 0.25 μm produced as a consequence of a standard breaking wave event, versus the oxygen saturation level, in percent, of the seawater in WST IV. Open circles indicate values obtained with 2-m-long Royco intake tube. Crosses indicate values obtained with 0.85-m-long tube. The solid curve corresponds to equation (1) in text.

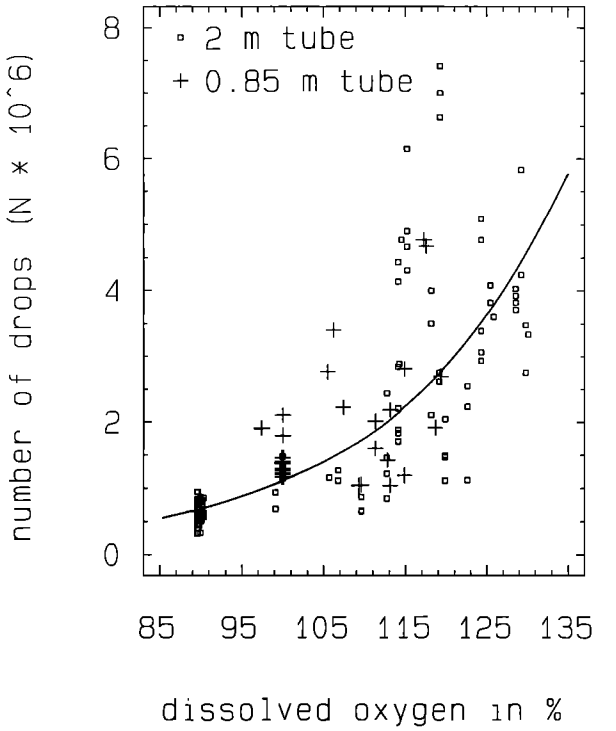

Fig. 5. Total number of droplets with radii greater than 2.5 μm produced as a consequence of a standard breaking wave event, versus the oxygen saturation level, in percent, of the seawater in tank. Open circles indicate measurements with 2-m-long intake tube. Crosses indicate measurements with 0.85-m-long tube. The solid curve corresponds to equation (2) in text.

creasing percentage saturation of the production of all droplets with radii greater than 0.25 μm. The variation in the ratio of $N(r > 2.5\ \mu m)$ to $N(r > 0.25\ \mu m)$ in response to changes in the percentage saturation, with respect to oxygen, of the sea water is given by

$$N(r > 2.5\mu m)N^{-1}(r > 0.25\mu m) = 0.01851 \exp(+0.0179s) \quad (3)$$

The profound effect of the seawater gas saturation level on the number of droplets generated during the decay of a standard whitecap having been determined, it was deemed appropriate to ascertain what, if any, influence gas saturation levels might have on the characteristic decay rates, as reflected in the associated e-folding times τ of individual whitecaps. Both τ and the number of droplets generated during the decay of a unit area of whitecap enter explicitly into the models that describe the rate of aerosol generation at the sea surface in terms of the instantaneous fraction of that surface covered by whitecaps [e.g., *Monahan et al.*, 1982, 1986].

The characteristic decay time associated with the exponential decay of the individual whitecaps [*Monahan and Zietlow*, 1969], as deduced from the analysis with a Hamamatsu area analyzer, model C1143-00, of a series of 18 video tape sequences taken with a Sony Trinicon video camera, model DXC1800P, mounted looking perpendicularly down at the center of WST IV from a vantage point 1.75 m above the still water surface, is given by

$$\tau = 0.268T_w - 0.912 \quad (4)$$

where τ is the characteristic decay time in seconds and T_w is the sea water temperature of degrees Celsius. The associated correlation coefficient is 0.92. The values of τ inferred from this equation, which range from 2.30 s for seawater at 12°C to 4.45 s for a water temperature of 20°C, span the characteristic decay time of 3.85 s obtained from the analysis of a sequence of still photographs taken of whitecaps in WST I [*Monahan and Zietlow*, 1969], the decay time of 3.53 s deduced from the analysis of cinefilm recordings of decaying whitecaps in WST II [*Monahan et al.*, 1982], and the decay time of 4.27 s recently obtained by *Nolan* [1988] from the analysis with the Hamamatsu area analyzer of nine full-scale oceanic whitecaps recorded in the North Sea during the 1986 HEXOS (Humidity Exchange Over the Sea) Main Experiment. The positive dependence of τ upon T_w embodied in (4) is in accord with the reasoning set forth by *Monahan and O'Muircheartaigh* [1986]. The rough similarity of these various values reflects the fact that all of these investigators were describing the same phenomenon, the decay of the coherent whitecap which is the surface manifestation of the mature bubble plume representing stage B in the evolution of the bubble cloud formed by a breaking wave [*Monahan* 1988*a*, *b*; *Monahan and Woolf*, 1989]. The observation that τ was, if anything, smaller when the oxygen saturation level was near 120% than it was when the saturation level was below 100% (the negative correlation coefficient for τ upon s was −0.88) supports the contention that the many small bubbles responsible for the massive late production of droplets in those cases where the water was markedly supersaturated with respect to dissolved oxygen do not contribute significantly to the optically resolvable surface whitecap.

Rather, these many small bubbles are the primary constituents of the stage C diffuse bubble cloud [*Monahan*, 1988*b*]. Thus it is this diffuse cloud of bubbles, clearly detected in the acoustic studies of near-surface bubble plumes [*Thorpe*, 1982, 1986*a*, *b*; *Thorpe and Hall*, 1983], whose lifetime should vary markedly with alterations in the level of oxygen saturation in the sea water.

CONCLUSIONS

The supersaturation of the seawater with respect to dissolved oxygen required for many of the measurements recorded in the preceding section was achieved by allowing the various batches of seawater, which were initially quite cold (having been drawn from Long Island Sound during the late autumn or winter), to warm up in WST IV in its relatively temperate laboratory. The highest degrees of supersaturation were attained during the early, quite rapid, stages of warming. Thus if the $N(r > 0.25\ \mu m)$ and $N(r > 2.5\ \mu m)$ values shown in Figures 4 and 5 were replotted versus seawater temperature, a strong negative correlation between the number of particles produced per breaking wave and seawater temperature would manifest itself. The immediate question to be answered then is whether the observed variations in droplet production are due primarily to the influence of the degree of saturation of the dissolved gases or are due in large part, or in whole, to some effect related to seawater temperature or to some temperature-dependent property such as kinematic viscosity. Fortunately, the variations in droplet production caused by changes in seawater temperature were investigated previously in a series of experiments that were carried out in WST II. The results of this earlier work were that the jet droplet production was typically seen to increase steadily with increasing seawater temperature, while the number of film droplets generated by a breaking wave usually showed little or no seawater temperature dependence over the range of temperatures (12.9°–23.5°C) encountered in the recent set of experiments [*Bowyer*, 1986; *Woolf et al.*, 1987]. In certain of the seawater samples used in some of the WST II experiments, the production of the small (i.e., film) droplets arising from a standard breaking wave was found to increase when the water temperature fell below some value, typically less than 15°C. But this change in film droplet production, when it occurred, was usually quite abrupt, has tentatively been attributed to a temperature induced change in the physical character of an organic surface film, and was not accompanied by any comparable variation in jet droplet production. It can thus be concluded that the variations in jet droplet and film droplet production illustrated in the preceding section of this paper are attributable to the recorded changes in the degree of gas saturation.

Since the solubilities of the major atmospheric gases decrease with increasing water temperature, in the recent experiments it was possible to attain the desired levels of supersaturation by simply allowing the seawater in WST IV to warm readily. Noting that the solubility in seawater of oxygen is some 49% greater at 5°C than at 25°C and that the solubility of nitrogen at 5°C is likewise some 43% greater than at 25°C [*Kester*, 1975], and observing that neither in the surface waters of Long Island Sound in late autumn and winter, nor in WST IV, were there levels of photosynthesis or of other biological processes that would greatly influence the dissolved oxygen concentration, it is reasonable to contend that the recorded oxygen supersaturation levels can be taken as an indication of the degree of nitrogen supersaturation as well. In order to assess the significance for global air-sea aerosol and moisture flux models of the findings described in the previous section as to the strong dependence of bubble-mediated aerosol production on the level of gas saturation, the range in the level of saturation of the surface waters of the world ocean with respect to dissolved oxygen and nitrogen must be considered.

In the absence of extensive records of dissolved nitrogen saturation levels, it is necessary to rely on the atlases and other compendiums that describe the dissolved oxygen content of the surface waters of the various oceans, recognizing that in certain regions and in certain seasons, photosynthesis and other biological processes will significantly influence the level of dissolved oxygen and thus make it in such instances a poor indicator of the nitrogen level. *Broecker and Peng* [1982] conclude that ocean surface waters are on average supersaturated with respect to oxygen by about 3%, and they present some data that document instances of 4%, and higher, supersaturations even in equatorial waters. While *Thorpe* [1984*a*] has suggested that 10-m-elevation winds of 16 m s^{-1} would be required to sustain, via bubble gas injection, oxygen and nitrogen supersaturations of 6.9%, data from the Antarctic Circumpolar region [*Gordon and Molinelli*, 1986] indicate that supersaturations of oxygen as great as 15% are not infrequently encountered. In regions off the California coast, where biological processes often are paramount in establishing the dynamics of gas exchange, dissolved oxygen levels have been recorded that range from 70% to 185% of the in situ equilibrium saturation values [*Simpson*, 1984].

The results obtained from the experiments described in this paper are applicable to the global ocean, as the salinity of the Long Island Sound water used in this work, while lower by several parts per thousand than the typical open ocean salinity, is well above the value at which the bubble spectrum arising from a breaking wave shifts from the spectrum characteristic of fresh water to that characteristic of seawater [*Scott*, 1975*a*, *b*].

The many more jet droplets that result from a standard breaking wave occurring in water that is markedly supersaturated with respect to dissolved oxygen (and nitrogen) than result when a similar wave breaks in water that is only saturated with these gases, are a consequence of many more small bubbles (with radii typically less than 100 μm) surviving to reach the surface in the case of supersaturation than in the case of mere saturation. The fate of small bubbles in unsaturated or even slightly supersaturated waters, i.e., the rapidity with which they go into solution, has been modeled in detail by *Thorpe* [1982, 1984*b*].

The question as to whether a wave breaking on the surface of an oceanic mixed layer supersaturated as regards the major atmospheric gases produces at the outset, by spontaneous nucleation and/or by other means, many more bubbles than the same breaking wave would produce if it occurred on the surface of a body of water just saturated with respect to these gases, is a matter yet to be resolved.

The initial practical application of the findings reported in this paper is in the refinement of the several previously published models describing, in terms of fractional oceanic whitecap coverage, the rate of bubble-mediated generation

of marine aerosol particles. One such model [*Monahan et al.*, 1986]

$$\partial F_0/\partial r = 3.58 \times 10^5 W r^{-3}(1 + 0.057 r^{1.05}) \times 10^{1.19\exp(-B^2)} \quad (5)$$

$$B = (0.380 - \log_{10} r)/0.650$$

represents the number of bubble-generated aerosol droplets produced per second, per unit area of sea surface, per increment of droplet radius, where these radii have been adjusted to the equilibrium radii these seawater droplets would attain in air at 80% relative humidity. In (5), W is the instantaneous fraction, not the percentage, of the ocean surface covered by coherent (stage B) whitecaps. In order to estimate W from measurements of the 10-m-elevation wind speed U, a statistically derived relationship, such as that obtained by *Monahan and O'Muircheartaigh* [1986] can be used:

$$W(U, \Delta T) = 1.95 \times 10^{-5} U^{2.55} \exp(0.861 \Delta T) \quad (6)$$

Here, U is expressed in meters per second and T, the water temperature minus the deck height air temperature, is given in degrees Celsius.

By taking the expression given in (2) as a measure of the effect of the saturation level, with respect to the major atmospheric gases, of the oceanic mixed layer on the production of jet droplets by breaking waves, a term $S(s)$,

$$S(s) = 9.10 \times 10^{-3} \exp(+0.0470 s)$$
$$S(s) = 1.00 \qquad s = 100\% \quad (7)$$

can be put forward as the first-order multiplicative correction to be applied to (5) to take into account the influence of the degree of gas saturation of the seawater on the production of jet droplets. In (7), s, the oxygen saturation level, is expressed in percent. The equation

$$\partial F_0/\partial r = 3.26 \times 10^3 W r^{-3}(1 + 0.057 r^{1.05}) \times 10^{1.19\exp(-B^2)} \exp(+0.0470 s) \quad (8)$$

obtained by combining (5) and (7), is thus the refined form of the earlier model of *Monahan et al.* [1986] for the generation of jet droplets at the sea surface.

At the conclusion of this paper it is appropriate to return to the conjecture about the effervescence of supersaturated sea water referred to in the introduction. The background aerosol concentrations measured within the hood of WST IV prior to a breaking wave event were typically higher when the seawater in the tank was markedly supersaturated than when it was near saturation, as can be seen from the traces in Figures 3*a* and 3*b*. Since these background counts were measured while filtered air was being continuously pumped through the hood and out its open second port, the higher background levels measured in the case of supersaturated waters must result from a continuous production of aerosol droplets within the tank in this case, as opposed to in the case of near-saturated waters. This clearly detectable production is in all probability the consequence of the surfacing of bubbles generated by the pumping necessary to elevate the water level behind the two water gates in preparation for the next breaking wave event. This being the case, it can be conjectured that even if still water that is markedly supersaturated does not spontaneously effervesce, sea water may nonetheless give off bubbles when subjected to the agitation, and pressure fluctuations, caused in nature by the wind and waves.

Acknowledgments. The laboratory investigations of bubble-mediated aerosol generation carried out at the University of Connecticut are supported by the Office of Naval Research via contract N00014-87-K-0185. The funds for the whitecap simulation tank IV were provided by the University of Connecticut Research Foundation. The authors gratefully acknowledge the invaluable assistance of M. B. Wilson in the conduct of the present experiments, and in the outfitting of WST IV and the associated laboratory. They wish to thank B. Welsh for the use throughout these experiments of her dissolved oxygen meter. Marine Sciences Institute, University of Connecticut, contribution 213.

REFERENCES

Blanchard, D. C., and A. H. Woodcock, Bubble formation and modification in the sea and its meteorological significance, *Tellus*, *9*, 145–158, 1957.

Blanchard, D. C., and A. H. Woodcock, The production, concentration, and vertical distribution of the sea-salt aerosol, *Ann. N. Y. Acad. Sci.*, *388*, 330–347, 1980.

Bowyer, P. A., Electrostatic phenomena associated with the marine aerosol arising from the bursting of whitecap bubbles, Ph.D. thesis, Nat. Univ. of Ireland, Dublin, 1986.

Broecker, W. S., and T.-H. Peng, *Tracers in the Sea*, 690 pp., Lamont-Doherty Geological Observatory, Palisades, N. Y., 1982.

Cipriano, R. J., E. C. Monahan, P. A. Bowyer, and D. K. Woolf, Marine condensation nucleus generation inferred from whitecap simulation tank results, *J. Geophys. Res.*, *92*, 6569–6576, 1987.

Garbalewski, C., and R. Marks, Dynamics of sea-spray populations in the lower air layer—Investigations during the 5th Antarctic Expedition to the H. Arctowski Station, *Pol. Polar Res.*, *6*, 415–436, 1985.

Gordon, A. L., and E. J. Molinelli, *Southern Ocean Atlas: Thermohaline and Chemical Distributions and the Atlas Data Set*, Amerind, New Delhi, 1986. (Available from Natl. Tech. Inf. Serv., Springfield, Va.)

Jacobs, W. C., Preliminary report on the study of atmospheric chlorides, *Mon. Weather Rev.*, *65*, 147–515, 1937.

Kester, D. R., Dissolved gases other than CO_2, in *Chemical Oceanography*, vol. 1, 2nd ed., edited by J. P. Riley and G. Skirrow, pp. 498–556, Academic, San Diego, Calif., 1975.

Kientzler, C. F., A. B. Arons, D. C. Blanchard, and A. H. Woodcock, Photographic investigation of the projection of droplets by bubbles bursting at a water surface, *Tellus*, *6*, 1–7, 1954.

Monahan, E. C., The ocean as a source for atmospheric particles, in *The Role of Air-Sea Exchange in Geochemical Cycling*, edited by P. Buat-Menard, pp. 129–163, D. Reidel, Hingham, Mass., 1986.

Monahan, E. C., Whitecap coverage as a remotely monitorable indication of the rate of bubble injection into the oceanic mixed layer, in *Sea Surface Sound*, edited by B. R. Kerman, pp. 85–96, Kluwer, Hingham, Mass., 1988*a*.

Monahan, E. C., Near-surface bubble concentration and oceanic whitecap coverage, paper presented at the Seventh Conference on Ocean-Atmosphere Interaction, Am. Meteorol. Soc., Anaheim, Calif., 1988*b*.

Monahan, E. C., and I. G. O'Muircheartaigh, Whitecaps and the passive remote sensing of the ocean surface, *Int. J. Remote Sens.*, *7*, 627–642, 1986.

Monahan, E. C., and D. K. Woolf, A comprehensive model relating the marine aerosol population of the atmospheric boundary layer to the bubble population of the oceanic mixed layer, in *Drops and Bubbles Colloquium Volume, A.I.P. Conf. Proc. Ser.*, pp. 451–457, American Institute of Physics, New York, 1989.

Monahan, E. C., and C. R. Zietlow, Laboratory comparisons of freshwater and salt-water whitecaps, *J. Geophys. Res.*, *74*, 6961–6966, 1969.

Monahan, E. C., B. D. O'Regan, and K. L. Davidson, Marine aerosol production from whitecaps, paper presented at XVII General Assembly, Int. Union of Geod. and Geophys., Canberra, Dec. 13, 1979.

Monahan, E. C., K. L. Davidson, and D. E. Spiel, Whitecap aerosol

productivity deduced from simulation tank measurements, *J. Geophys. Res.*, *87*, 8898–8904, 1982.

Monahan, E. C., D. E. Spiel, and K. L. Davidson, A model of marine aerosol generation via whitecaps and wave disruption, in *Oceanic Whitecaps and Their Role in Air-Sea Exchange Processes*, edited by E. C. Monahan and G. MacNiocaill, pp. 167–174, D. Reidel, Hingham, Mass., 1986.

Nolan, P. F., Decay characteristics of individual whitecaps, Oceanic Whitecaps and the Fluxes of Droplets from, Bubbles to, and Gases Through the Sea Surface, *Whitecap Rep. 4*, edited by E. C. Monahan, R. J. Cipriano, W. F. Fitzgerald, R. Marks, R. Mason, P. F. Nolan, T. Torgersen, M. B. Wilson, and D. K. Woolf, pp. 41–56, Mar. Sci. Inst., Univ. of Conn., Avery Point, 1988.

Scott, J. C., The preparation of water for surface-clean fluid mechanics, *J. Fluid Mech.*, *69*, 339–351, 1975*a*.

Scott, J. C., The role of salt in whitecap persistence, *Deep Sea Res.*, *22*, 653–657, 1975*b*.

Simpson, J. J., On the exchange of oxygen and carbon dioxide between ocean and atmosphere in an eastern boundary current, in *Gas Transfer at Water Surfaces*, edited by W. Brutsaert and G. J. Jirka, pp. 505–514, D. Reidel, Hingham, Mass., 1984.

Stramska, M., Vertical profiles of sea-salt aerosol: A numerical model, *Acta Geophys. Pol.*, *35*, 87–100, 1987.

Thorpe, S. A., On the clouds of bubbles formed by breaking wind-waves in deep water, and their role in air-sea gas transfer, *Philos. Trans. R. Soc., London, Ser. A*, *304*, 155–210, 1982.

Thorpe, S. A., The role of bubbles produced by breaking waves in supersaturating the near-surface ocean mixing layer with oxygen, *Ann. Geophys.*, *2*, 53–56, 1984*a*.

Thorpe, S. A., A model of the turbulent diffusion of bubbles below the sea surface, *J. Phys. Oceanogr.*, *14*, 841–854, 1984*b*.

Thorpe, S. A., Bubble clouds: A review of their detection by sonar, of related models and of how K_v may be determined, in *Oceanic Whitecaps and Their Role in Air-Sea Exchange Processes*, edited by E. C. Monahan and G. MacNiocaill, pp. 57–68, D. Reidel, Hingham, Mass., 1986*a*.

Thorpe, S. A., Measurements with the automatically recording inverted echo sounder; ARIES and the bubble clouds, *J. Phys. Oceanogr.*, *16*, 1462–1478, 1986*b*.

Thorpe, S. A., and A. J. Hall, The characteristics of breaking waves, bubble clouds, and near-surface currents observed using side-scan sonar, *Cont. Shelf Res.*, *1*, 353–384, 1983.

Woolf, D. K., P. A. Bowyer, and E. C. Monahan, Discriminating between the film drops and jet drops produced by a simulated whitecap, *J. Geophys. Res.*, *92*, 5142–5150, 1987.

Woolf, D. K., E. C. Monahan, and D. E. Spiel, Quantification of the marine aerosol produced by whitecaps, paper presented at the Seventh Conference on Ocean-Atmosphere Interaction, Am. Meteorol. Soc., Anaheim, Calif., 1988.

R. Marks, E. C. Monahan, and M. Stramska, Marine Sciences Institute, University of Connecticut, Avery Point, Groton, CT 06340.

(Received June 1, 1989;
revised December 14, 1989;
accepted January 8, 1990.)